

# NUMERICAL MODELLING OF CIRCULAR CONCRETE COLUMNS STRENGTHENED WITH HYBRID FRP JACKETS

J. V. Matias, E. Júlio, N. Silvestre

**Abstract.** This paper presents a nonlinear finite element model that accurately simulates the behaviour of circular concrete columns strengthened with jackets of hybrid multilayer FRP fabrics and loaded in compression. The research focus is on the strength and ductility enhancement provided by this innovative confinement system. First, a brief literature review on FRP-wrapped concrete is presented. Next, the experimental work adopted to calibrate and validate the present study is shortly described. Then, the numerical model is presented, and comparisons between experimental and numerical results are made, validating the proposed model. It is concluded that the plasticity model can be used to numerically simulate concrete confined by FRP jacketing with hybrid systems with good agreement for stress-strain curves and failure modes. The influence of the ultimate strain on the confinement of the concrete core is assessed corroborating that, for higher values of fibres' ultimate strain, better confinement is achieved.

**Keywords:** concrete, columns, confinement, strengthening, FRP jacketing, hybrid systems, finite element method, plasticity model

## 1. Introduction

Existing concrete structures often need repair and/or rehabilitation, mostly due to deterioration caused by environmental attack or due to extreme events or changes in design assumptions. Concrete columns are usually strengthened using concrete jacketing since this leads to an enhancement in both ductility and strength. Presently, fibre reinforced polymer (FRP) jacketing is an interesting alternative to the latter, for its high strength-to-weight ratio, simple application procedure, and irrelevant geometry increase. In this section, a brief review of studies conducted on this strengthening technique, focusing on confinement, is presented.

In early studies on FRP wrapping of concrete columns, the stress-strain model of Mander *et al.* [1, 2] for steel-confined concrete was used to predict its behaviour [3]. However, some

deviations were found, mainly due to the fact that the latter considers a constant confining pressure, which is a good assumption for the steel-confined concrete but apparently not for FRP-wrapping. In this case an increasing confining pressure is observed until failure of the FRP sheets is reached.

In the past two decades many empirical or semi-empirical models [4, 5, 6, 7, 8, 9] for circular columns were proposed, based on experimental test data. However, these were typically calibrated with a reduced number of specimens and conditions, therefore leading to good results only in limited situations. Comparative studies conducted by De Lorenzis and Tepfers [10] revealed that, in average, there was an error higher than 13% and 35%, respectively for strength and ductility predictions, thus clearly showing the need for a deeper study on the behaviour of concrete confined with FRP jacketing. Another

influencing parameter, also contributing to the deviations referred to, is the confinement provided by the steel (transversal and longitudinal) reinforcing bars of the existing concrete column / specimen.

Constitutive models for FRP wrapped concrete columns are characterized in general by a bilinear behaviour. The initial part of the slope is very similar to that of the unconfined concrete, since the confinement only takes place when the tensile strength of the concrete is reached. For this reason, this first part is only influenced by concrete characteristics. When concrete's tensile strength is reached, concrete starts expanding mobilizing the FRP sheets (see **Erro! A origem da referência não foi encontrada.. a)** leading to an increase in the confinement pressure of the concrete core. That leads to a second linear part of the slope, which is mainly characterized by the FRP properties (see **Erro! A origem da referência não foi encontrada.. b).**

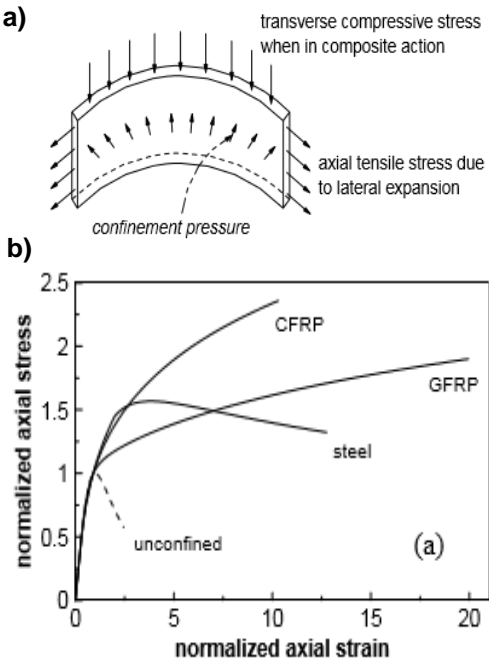


Fig. 1. a) FRP jacket stress behaviour [12] b)

Stress-strain curves for different jacketing materials [12]

Finite element models, being able of adapting to different conditions and complex stress variations in concrete, are widely used to predict the confined behaviour of concrete. Many constitutive models have been studied, including plasticity models, plastic-damage models and elastic-damage models. Plasticity models, such as the Drucker-Prager model, have shown the best results for modelling confined concrete, and several authors have applied it to model external FRP-wrapped concrete columns [13, 14, 15].

Recently other hybrid (or bistable) retrofitting solutions using FRP have been studied, consisting of layers of two different type of FRP sheets instead of only one type. The main purpose for that solution is to use characteristics of different fibres, such as using one with higher tensile strength and another with higher ultimate strain, this way ensuring that after one reaches its tensile strength the other can still resist. This idea has been first presented by Cherkaev and Slepian [16], designating the first as “main link” and the other as “waiting link”. Another reason for adopting this solution is a wider range of possible elastic modulus of the FRP jacketing solution, leading to a greater range of confinement pressures. Nevertheless, this hybrid solution still needs further investigation, since only few studies have already been conducted [17, 18].

The main goal of the study herein described was to build and calibrate numerical models for circular hybrid FRP-wrapped short columns using stress-strain curves and failures modes of the experimental study conducted by

Henriques [19] and, with these, to contribute to a better knowledge of the behaviour of concrete columns confined with this strengthening technique.

## 2. Experimental Tests

In this section, a brief description of the experimental tests conducted by Henriques [18], used to calibrate the numerical models, is presented.

### 2.1. Experimental Program

Monotonic axial compression tests were performed, up to failure, on 12 different series of 3 layers FRP-wrapped concrete columns with circular cross-section with 150 mm in diameter and 300 mm in length. For each situation, 2 equal specimens were produced. From the 12 series, 4 of them corresponded to current FRP jacketing, i.e., with all layers from the same fibre type, and 8 of them corresponded to the innovative hybrid systems, i.e., with layers varying in fibre type and order. Four types of fibres were used: low modulus carbon (C<sub>1</sub>), high modulus carbon (C<sub>2</sub>), aramid (A), and glass (G). Tests were performed using a 3000 kN load-capacity *walter+bay* testing machine.

Two different group of tests were performed with different concrete characteristics, named PB<sub>1</sub> and PB<sub>2</sub>. In Table 1 the different series and fibre type combinations are listed. Taking the first specimen, PB<sub>1</sub>.3C<sub>1</sub>, to illustrate the adopted specimen label: 'PB<sub>1</sub>' refers to the first group of tests and '3C<sub>1</sub>' means that three layers of low modulus carbon have been used.

Table 1. FRP jacketing configuration for each series of tests (adapted from [19])

Group	Series	FRP jacketing configuration
-------	--------	-----------------------------

	First Layer	Second Layer	Third Layer	
1	PB <sub>1</sub> .3C <sub>1</sub>	Carbon (C <sub>1</sub> )	Carbon (C <sub>1</sub> )	Carbon (C <sub>1</sub> )
	PB <sub>1</sub> .3C <sub>2</sub>	Carbon (C <sub>2</sub> )	Carbon (C <sub>2</sub> )	Carbon (C <sub>2</sub> )
	PB <sub>1</sub> .C <sub>1</sub> .2C <sub>2</sub>	Carbon (C <sub>1</sub> )	Carbon (C <sub>2</sub> )	Carbon (C <sub>2</sub> )
	PB <sub>1</sub> .2C <sub>1</sub> .C <sub>2</sub>	Carbon (C <sub>1</sub> )	Carbon (C <sub>1</sub> )	Carbon (C <sub>2</sub> )
	PB <sub>1</sub> .C <sub>1</sub> .2A	Carbon (C <sub>1</sub> )	Aramid (A)	Aramid (A)
	PB <sub>1</sub> .2C <sub>1</sub> .A	Carbon (C <sub>1</sub> )	Carbon (C <sub>1</sub> )	Aramid (A)
	PB <sub>1</sub> .A.C <sub>1</sub> .A	Aramid (A)	Carbon (C <sub>1</sub> )	Aramid (A)
	PB <sub>1</sub> .2A.C1	Aramid (A)	Aramid (A)	Carbon (C <sub>1</sub> )
2	PB <sub>2</sub> .3A	Aramid (A)	Aramid (A)	Aramid (A)
	PB <sub>2</sub> .3G	Glass (G)	Glass (G)	Glass (G)
	PB <sub>2</sub> .2A.G	Aramid (A)	Aramid (A)	Glass (G)
	PB <sub>2</sub> .A.2G	Aramid (A)	Glass (G)	Glass (G)

### 2.2. Material Properties

As previously mentioned, two concrete mixes were used, cast at different times. To characterize these, concrete columns without reinforcement were tested (see Table 2).

Table 2. Concrete properties according to Henriques [19]

	f <sub>cm,cil</sub> (MPa)	f <sub>cm,cub</sub> (MPa)	ε <sub>c1</sub> (%)	E <sub>cm</sub> (GPa)
PB <sub>1</sub>	34.40	43.00	0.21	30.669
PB <sub>2</sub>	31.80	39.75	0.21	29.954

The following unidirectional FRP sheets were used to strengthen the concrete columns: S&P C-Sheet 240, *Low Modulus Carbon Fibre Reinforced Polymer* (C<sub>1</sub>FRP), S&P C-Sheet 640, *High Modulus Carbon Fibre Reinforced Polymer* (C<sub>2</sub>FRP) and S&P A-Sheet 120, *Aramid Fibre Reinforced Polymer* (AFRP). In addition, the following bidirectional FRP sheet

was also used: S&P G-Sheet AR 90/10 type B, *Glass Fibre Reinforced Polymer (GFRP)*. The properties (Young's modulus,  $E_f$ , and thickness,  $t$ ) of these FRP sheets were provided by the manufacturer and are shown in Table 3.

Table 4. FRP sheets properties [20]

	CFRP		AFRP (A)	GFRP (G)
	LM (C <sub>1</sub> )	HM (C <sub>2</sub> )		
$E_f$ (GPa)	240	640	120	65
$t$ (mm)	0.176	0.190	0.200	0.299

To bond the FRP sheets to the concrete surface an epoxy resin from the same manufacturer, S&P Resin 55, was used.

### 2.3. Test Results

Tests confirmed that the stress-strain behaviour of FRP-wrapped concrete columns is clearly bilinear (see Fig. 2), for both current and hybrid retrofitting, as assumed in different analytical models [4, 5, 6, 7, 8, 9]. Concrete confinement provided by FRP jackets enabled a higher ultimate stress and strain, varying with the adopted FRP configuration.

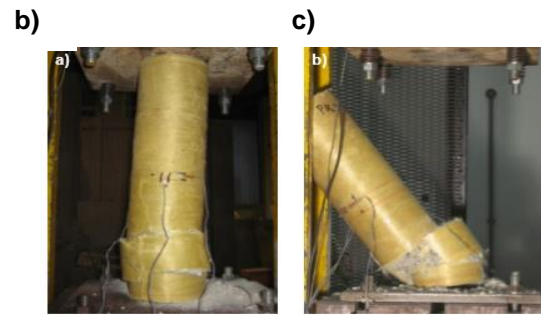
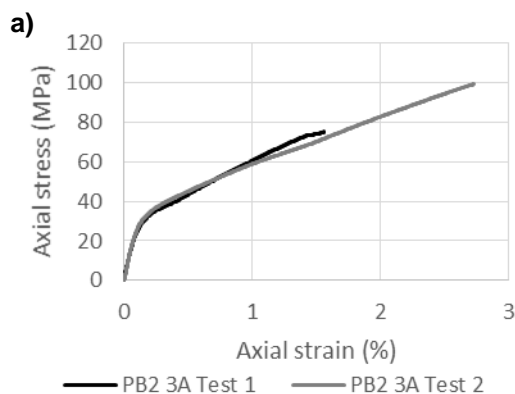


Fig. 2. a) Stress-strain behaviour registered for both PB<sub>2.3A</sub> tests; b) Failure mode of the first specimen; c) Failure mode of the second specimen

Regarding the columns strengthened with only one type of fibres, AFRP was the one exhibiting better improvements ( $f_{cc}/f_{c0}=2.8$ ), followed by GFRP ( $f_{cc}/f_{c0}=2.2$ ), and lastly both CFRP sheets ( $f_{cc}/f_{c0}=1.6$ ).

Regarding hybrid systems, combination of AFRP and GFRP presented the best results ( $f_{cc}/f_{c0}=2.5$  and  $2.7$ ), followed by AFRP and C<sub>1</sub>FRP ( $f_{cc}/f_{c0}=2.0$  and  $2.2$ ), and lastly again both CFRP hybrid systems ( $f_{cc}/f_{c0}=1.5$  and  $2.0$ ). In terms of ductility, AFRP and C<sub>1</sub>FRP hybrid systems have shown the best results.

The results proved that the improvements of FRP-wrapped columns are directly related to the ultimate strain of the adopted FRP system, being the best results achieved with fibres with a higher ultimate strain.

### 3. Finite element modelling

To accurately simulate the behaviour of FRP-wrapped columns, it is necessary to properly assess the element type and mesh, as well as the constitutive law, for each material involved. As previously referred to, modelling confined concrete is the most complex aspect of this study. The finite element commercial package

ABAQUS [21] was selected to generate the models.

### 3.1. Finite element type and mesh

Different types of elements have been studied regarding confined concrete columns strengthened with FRP jacketing or other solutions. In studies conducted on modelling of confined concrete in short concrete-filled steel columns [22, 23] and FRP-wrapped columns [14], it was concluded that 3-D 8-node solid elements (C3D8) are the most effective. This is due to the concrete core deformation characteristics when subjected to axial compression without rotation [22].

Since the thickness of the FRP sheets is much smaller than the other dimensions, the jackets act like a shell, thus a 4-node shell (S4) elements were adopted to model these, as previously done in similar studies [17]. Being the aim of this work to study the behaviour of FRP hybrid systems, there was a need to model the different layers separately. For this reason, a composite layup conventional shell was adopted, where each FRP sheet was modelled as a different ply (see Fig. 3). The epoxy-based bonding agent was not considered due to its lower stiffness and also aiming at not turning the analysis too complex.

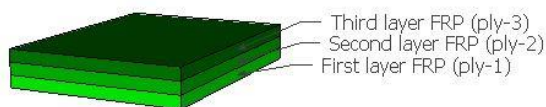


Fig. 3. Composite layup conventional shell scheme used

The loading system included two rigid plates at both ends of the concrete column. To model these plates, C3D8 elements and a rigid body constraint function were used.

Regarding the mesh size, a 10 mm spacing was adopted for concrete and 5 mm for FRP. These values were defined considering previous studies on short concrete-filled steel columns [22]. Compared to the concrete core, a more refined mesh (circa half the size) was used for the FRP jacket, to guarantee a good adjustment at the curved contact surface.

In Fig. 4 the mesh adopted for the concrete core and the mesh adopted for the FRP jacketing are presented.

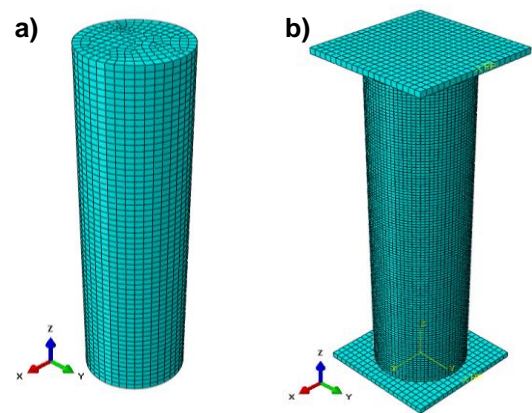


Fig. 4. Finite elements mesh of the a) concrete core and b) FRP jacket and end plates.

### 3.2. Boundary conditions and loading

Boundary conditions were settled for the top and bottom rigid plates. All degrees of freedom were restrained except for the displacement at the loaded end, i.e. the vertical direction of the top plate.

Interactions were considered between both rigid plates and the concrete core, and the FRP jackets and the concrete core. Regarding the first, a mechanical contact interaction was used, with a friction coefficient of 0.25 for the tangential behaviour and a normal “hard” contact behaviour, as adopted in [22, 23]. Regarding the second, a constraint tie was

used, corresponding to perfect bonding between both elements.

The load was applied in increments, using a static general analysis since nonlinear post-buckling behaviour was not expected to occur.

### 3.3. Material modelling of confined concrete

Modelling of confined concrete is quite complex due to its cracking propagation unpredictability. A plasticity approach was used to model its behaviour, namely the *Concrete Damaged Plasticity* (CDP) model of ABAQUS [21], which uses a non-associated plastic flow potential based on the Drucker-Prager hyperbolic function, given by Eq. (1):

$$G = \sqrt{(ef_{ctm}\tan\varphi)^2 + q^2} - p\tan\varphi \quad (1)$$

where  $e$  is the flow potential eccentricity of the hyperbolic function (taken herein as  $e = 0.1$  by default),  $\Psi$  is the dilation angle,  $q$  is the von Mises equivalent effective stress, and  $p$  is the hydrostatic pressure. A similar approach has been adopted by other authors to model different types of passive confinement of concrete [24, 25]. The CDP model uses two additional parameters, the ratio of initial equibiaxial compressive yield stress to initial uniaxial compressive yield stress ( $f_{b0}/f_{c0}$ ), by default equal to 1.16, and the ratio of the second stress invariant on the tensile meridian to that on the compressive meridian ( $K_c$ ), by default equal to 2/3 [21]. The dilation angle used for both concrete mixes was 20°, for having shown good results in different confined concrete models [23].

In addition to the parameters referred to, the CDP model requires the definition of the stress-strain curves of concrete when

subjected to uniaxial compression and tension. To define the compression curves, using the *Concrete Compression Hardening* [21] command as part of the CDP model, the curve was separated into two different branches. First, for the hardening ascending branch, the expressions from Eurocode 2 part 1-1 [26] to the unconfined concrete behaviour (Eq. 2-4) were used:

$$f_c = f_{cm,cyl} \frac{k\eta - \eta^2}{1 + (k - 2)\eta} \quad (2)$$

$$\eta = \frac{\varepsilon}{\varepsilon_c} \quad (3)$$

$$k = 1.05E_{cm} \frac{\varepsilon_c}{f_{cm,cyl}} \quad (4)$$

where  $f_c$  is the concrete stress,  $f_{cn,cyl}$  is the equivalent cylinder concrete compressive strength (Table 2),  $E_{cm}$  is the concrete's Young's modulus (Table 2), and  $\varepsilon_c$  is the concrete strain (Table 2).

For the second branch (descending), a linear behaviour was used, with a value of  $0.9f_{cn,cyl}$ , corresponding to an axial strain equal to 0.01. This approach has been used by other authors to model the behaviour of confined concrete, with good results [22, 23, 25]. In Fig. 5 the curves corresponding to each concrete mix used by Henriques [19] are shown.

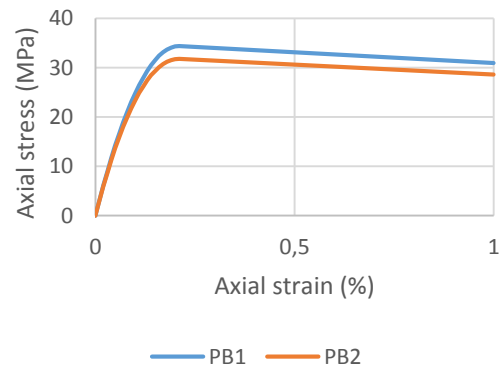


Fig. 5. Stress-strain curves for concrete subjected to compression used in the model

When modelling confined concrete, the tensile behaviour usually is of less importance. Nevertheless, to define this behaviour, the *Concrete Tension Stiffening* [21] command has been used, assuming a simple approach based on crack opening displacement. A value of 3 MPa was adopted for the splitting tensile strength ( $f_{ctm}$ ), and a linear behaviour up to this value was assumed. After reaching the splitting tensile strength, the stress varies linearly to zero until an ultimate cracking displacement of 0.08mm is reached [21].

### 3.4. Material modelling of FRP

FRP jackets are composed by i) fibres, that are responsible for the structural properties, namely strength and elasticity, ii) matrix, that is responsible for maintaining a uniform behaviour, and iii) epoxy resin, that bonds the FRP sheets to the concrete surface. It is known that the fibres behaviour is quite anisotropic, exhibiting high strength and high Young's modulus only in the main direction.

FRP was defined as an elastic material with a Young's modulus presented in Table 4 according to the main direction, which is the hoop direction in this case. In the other directions, values of lower magnitude were used (circa 5 GPa). Thickness and fibre direction are specified in the conventional shell characteristics of the composite layup, being the direction chosen the hoop direction.

## 4. Numerical results and discussion

In order to check and calibrate the finite element model, a comparison with the experimental results obtained by Henriques [19] was made. Stress-strain curves were compared and deformed shapes analysed.

It is known that stress-strain curves of FRP-wrapped concrete are usually characterized by a bilinear behaviour. In different analytical models, two slopes are used to describe the stress-strain curves: i) a first branch slope,  $E_I$ , conditioned mainly by the unconfined concrete characteristics, and ii) a second branch slope,  $E_{II}$ , mainly conditioned by the FRP confinement behaviour.

Regarding  $E_I$ , the model showed good agreement with the experimental results for most cases (see Fig. 6), being the major differences due to the variability inherent to experimental tests (especially for the first concrete mix).

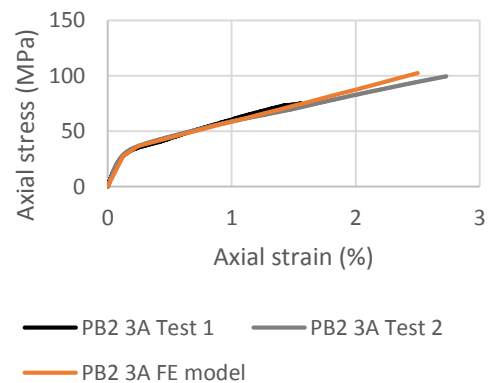


Fig. 6. Comparison between experimental and numerical results for the PB<sub>2</sub>.3A series

Regarding  $E_{II}$ , generally a good agreement was also achieved between experimental and numerical results (see Fig. 7). However, major differences were registered in the case of columns strengthened with CFRP. According to Henriques [19], this may be due to the fact that the ultimate strain of CFRP was lower than expected. Therefore, the FRP jacketing was unable to adequately confine the concrete core, and lower values were achieved. Some differences can be seen as well on the PB<sub>2</sub>.3G and PB<sub>2</sub>.1A.2G series but, in these cases,

higher values are reached. Another reason that may explain this behaviour is the fact that the model did not consider the epoxy resin.

Depending on the value of the epoxy resin thickness, even for a lower Young's modulus, this can significantly influence results.

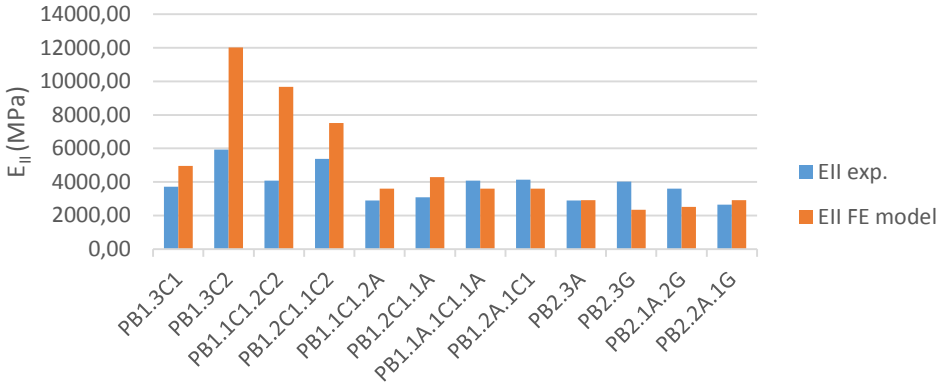


Fig. 7. Comparison of second slope from the average values obtained by Henriques [19] and FE models

Lastly, the deformed shape was analysed and compared with the failure modes observed by Henriques [19]. As shown in Fig. 8, columns' failure was observed when failure of the FRP sheets occurred. Analysing the deformed shape of the FE model, a higher lateral expansion is observed at a quarter of the height, near the top or the bottom ends, exactly where in the tested specimens failure was registered.

### 5. Conclusions

In this paper, a numerical study conducted to study the behaviour of circular concrete columns strengthened with hybrid FRP systems is described. Firstly, a brief state-of-the-art review on FRP-wrapped concrete columns and confined concrete is presented, as well as a short description of the experimental tests performed by Henriques [19]. Then, nonlinear finite element models of FRP-wrapped concrete columns built using ABAQUS [21] are described, as well as a method to model the behaviour of confined concrete. Lastly, comparisons between experimental and numerical results are discussed and the following main conclusions are drawn:

- The model adopted in this work to simulate the behaviour of concrete confined with FRP jacketing revealed a good agreement with experimental data. The *Concrete Damaged Plasticity* model proved to be able of

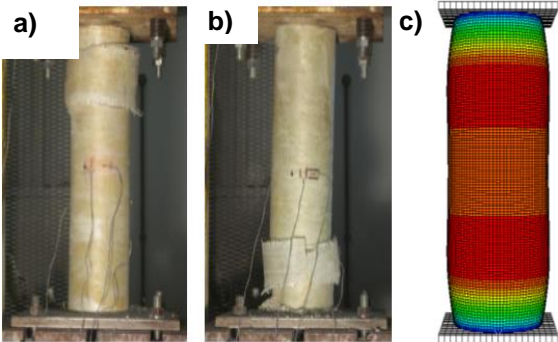


Fig. 8. a) Failure mode of the first specimen from the PB<sub>2</sub>.2A.1G series, b) Failure mode of the second specimen from the PB<sub>2</sub>.2A.1G series, and c) Deformed shape of the FE model of the PB<sub>2</sub>.2A.1G series



modelling the inelastic behaviour of concrete confined by FRP-wrapping;

- The models were validated with the comparison of the numerical and experimental results, including stress-strain curves and deformed shapes/failure modes. The influence of the type of sheets used on the FRP jackets in the concrete confinement were numerically observed;
- Results shown that the numerical models used tend to overestimate the ultimate axial stress obtained for columns strengthened with carbon fibres with higher elastic modulus and lower ultimate strain (shown by the second branch slope  $E_{II}$ ). This reveals that the concrete confinement behaviour in FRP-wrapped concrete columns is not fully achieved, as in perfect conditions considered in the numerical models, possible due to FRP jackets with higher elastic modulus not being able to generate the expected lateral stress.
- Numerical models of hybrid solutions with low modulus carbon ( $C_1$ ) and aramid (A) shown that the order of which the FRP sheets were applied had no influence on the overall behaviour and resistance of the strengthened concrete column.
- Models of concrete columns strengthened with different hybrid AFRP sheets shown a better approach to the experimental results. This shown that AFRP-wrapped concrete columns achieve a confined concrete state closer to a perfect bounding conditions considered on the

numerical models. For FRP sheets with higher ultimate strains, a more effective confining pressure is achieved, enhancing the concrete core characteristics.

## References

- [1] J. B. Mander, M. J. N. Priestley and R. Park, "Theoretical Stress-Strain Model for Confined Concrete," *J. Struct. Engrg., ASCE*, vol. 114(8), pp. 1804-1826, 1988.
- [2] M. N. Fardis and H. Khalili, "Concrete encased in fibre glass reinforced plastic," *American Concrete Institute Journal*, vol. 6, pp. 440-446, 1981.
- [3] H. Saadatmanesh, M. R. Ehsani and M. W. Li, "Strenght and Ductility of Concrete Columns Externally Reinforced with Fibre Composites Straps," *ACI Structural Journal*, vol. 91, pp. 434-447, 1994.
- [4] S. M. Ahmad, A. R. Khaloo and A. Irshaid, "Behavior of concrete spirally confined by fibreglass filaments," *Magazina of Concrete Research*, vol. 156, pp. 143-148, 1991.
- [5] M. Saaman, A. Mirmiran and M. Shahawy, "Model of Concrete Confined by Fibre Composites," *Journal of Structural Engineering, ASCE*, vol. 9, pp. 1025-1031, 1998.
- [6] A. Mirmiran, M. Shahawy, M. Saaman, H. El Achary, J. Mastrapa and J. Pico, "Effect of columns parameters on FRP-Confined Concrete," *Journal of Composites for Construction*, vol. 4, pp. 175-185, 2007.
- [7] M. Spoelstra and G. Monti, "FRP-Confined Concrete Model," *Journal of Composites for Construction, ASCE*, vol. 3, pp. 143-150, 1999.
- [8] Y. Wei and Y. Wu, "Unified stress-strain model of concrete for FRP-confined columns,"

- Construction and Building Materials*, vol. 26, pp. 381-392, 2012.
- [9] C.-D. 200/2004, Guide for the Design and Construction of Externally Bonded FRP Systems for Strengthening Existing Structures, National Research Council, Rome, 2004.
- [10] L. De Lorenzis and R. Teffers, "Comparative studies of models on confinement of concrete cylinders with fibre-reinforced polymer composites," *Journal of composites for construction*, ASCE, pp. 219-237, 2003.
- [11] J. Teng and L. Lam, "Behavior and modeling of fibre reinforced polymer-confined concrete," *J. Struct. Eng.*, vol. 130(11), pp. 1713-1723, 2004.
- [12] F. b. 14, Externally bonded FRP reinforcement for RC structures, Fédération Internationale du Béton (fib), Task Group 9.3 FRP, Lausanne, 2001.
- [13] T. T. J. G. Yu, Y. L. Wong and S. L. Dong, "Finite element modeling of confined concrete-I: Drucker-Prager type plasticity model," *Engineering Structures*, vol. 32, pp. 665-679, 2010.
- [14] A. I. Karabinis, T. C. Rousakis and G. E. Manolitsi, "3D finite-element analysis of substandard RC columns strengthened by fibre-reinforced polymer sheets," *Journal of Composites for Construction*, vol. 12, pp. 531-540, 2008.
- [15] A. Mirmiran, K. Zagers and W. Yuan, "Nonlinear finite element modeling of concrete confined by fibre composites," *Finite Elements in Analysis and Design*, vol. 35, pp. 79-96, 2000.
- [16] A. Cherkaev and L. Slepian, "Waiting element structures and stability under extension," *International Journal of Damage Mechanics*, vol. 4, pp. 58-82, 1995.
- [17] C. Quon, L. Cheng, Y. Li and W. Yu, "Confinement of concrete with hybrid FRP bistable structures," *Cement & Concrete Composites*, Elsevier, vol. 37, pp. 222-231, 2013.
- [18] C. Wan, L. Cheng, Y. Li and W. Yu, "Confinement of concrete with hybrid FRP bistable structures," *Cement & Concrete Composites*, Elsevier, vol. 37, pp. 222-231, 2013.
- [19] S. Henriques, Reforço de Pilares de Betão por Encamisamento Híbrido com Mantas de FRP, 2016.
- [20] S&P Data Sheets.
- [21] ABAQUS, User's Manual, Rhode Island, USA: Standard, Simulia, 2010.
- [22] X. Dai and D. Lam, "Numerical modelling of the axial compressive behaviour of short," *Journal of Constructional Steel Research* 66(7) , pp. 931-942, 2010.
- [23] E. Ellobody, B. Young and D. Lam, "Behaviour of normal and high-strength concrete-filled compact steel tube circular stub columns," *Journal of Constructional Steel Research* 62 , pp. 706-715, 2006.
- [24] S. P. Schneider, "Axially loaded concrete-filled steel tubes," *Journal of Structural Engineering*, ASCE, vol. 124(10), pp. 1125-1138, 1998.
- [25] A. P. C. Duarte, N. Silvestre, J. de Brito, E. Júlio and J. M. Castro, "Finite Element Modelling of Short Steel Tubes Filled with Rubberized Concrete," *Composite Structures*, p. (em revisão), 2016.
- [26] CEN, EN 1992-1-1, Eurocode 2: Design of concrete structures - Part 1-1: General rules and rules for buildings, European Committee for Standardization, Brussels, Belgium, 2010.

